

1 Thermostability Engineering of a Class II Pyruvate Aldolase from 2 *Escherichia coli* by *in Vivo* Folding Interference

3 Sandra Bosch, Esther Sanchez-Freire, María Luisa del Pozo, Morana Česnik, Jaime Quesada,
4 Diana M. Mate, Karel Hernández, Yuyin Qi, Pere Clapés, Đurđa Vasić-Rački, Zvezdana Findrik Blažević,
5 José Berenguer, and Aurelio Hidalgo*



Cite This: <https://doi.org/10.1021/acssuschemeng.1c00699>



Read Online

ACCESS |



Metrics & More



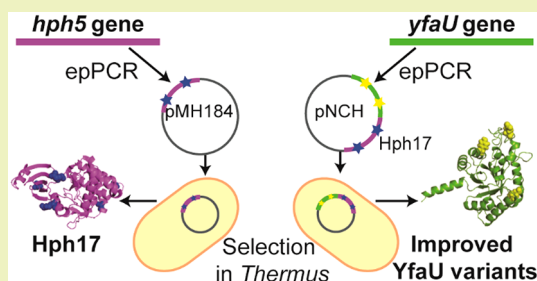
Article Recommendations



Supporting Information

6 **ABSTRACT:** The use of enzymes in industrial processes is often limited by
7 the unavailability of biocatalysts with prolonged stability. Thermostable
8 enzymes allow increased process temperature and thus higher substrate and
9 product solubility, reuse of expensive biocatalysts, resistance against organic
10 solvents, and better “evolvability” of enzymes. In this work, we have used an
11 activity-independent method for the selection of thermostable variants of any
12 protein in *Thermus thermophilus* through folding interference at high
13 temperature of a thermostable antibiotic reporter protein at the C-terminus
14 of a fusion protein. To generate a monomeric folding reporter, we have
15 increased the thermostability of the moderately thermostable Hph5 variant of
16 the hygromycin B phosphotransferase from *Escherichia coli* to meet the
17 method requirements. The final Hph17 showed 1.5 °C higher melting temperature (T_m) and 3-fold longer half-life at 65 °C
18 compared to parental Hph5, with no changes in the steady-state kinetic parameters. Additionally, we demonstrate the validity of the
19 reporter by stabilizing the 2-keto-3-deoxy-rhamnonate aldolase from *E. coli* (YfaU). The most thermostable multiple-mutated
20 variants thus obtained, YfaU99 and YfaU103, showed increases of 2 and 2.9 °C in T_m compared to the wild-type enzyme but severely
21 lower retro-aldol activities (150- and 120-fold, respectively). After segregation of the mutations, the most thermostable single variant,
22 Q107R, showed a T_m 8.9 °C higher, a 16-fold improvement in half-life at 60 °C and higher operational stability than the wild-type,
23 without substantial modification of the kinetic parameters.

24 **KEYWORDS:** aldolase, directed evolution, hygromycin B phosphotransferase, *in vivo* selection, thermostability, *Thermus thermophilus*



25 ■ INTRODUCTION

26 Reaction conditions of enzymes in industrial biocatalysis are
27 usually far from those in nature: non-natural substrates are
28 used in high concentrations while higher temperatures and
29 organic cosolvents are needed to promote substrate and
30 product solubility. In this context, enzyme engineering
31 constitutes an efficient methodology to tailor enzyme activity,
32 substrate selectivity, or stability under operational conditions
33 to each industrial process.¹

34 The rational prediction of thermostability is a complex task
35 because methods are based on different structure–function
36 hypotheses, leading to different solutions, which in many cases
37 do not result in direct increases in stability.² Therefore,
38 directed evolution is preferred, since it allows exploration of a
39 large sequence space (in the range of 10⁶ to 10⁹ individuals),³
40 albeit at the cost of increasing the screening effort to cover a
41 meaningful fraction of this man-made diversity.

42 Screening for thermostable enzyme variants in large libraries
43 can be carried out in a thermophile, provided its growth is
44 coupled to the stability of the target protein.⁴ In 2007, we
45 reported a procedure for the *in vivo* selection of thermostable
46 variants of any protein independently of its activity using

Thermus thermophilus as a host.⁵ The method was based on the 47
48 folding interference phenomenon that occurs in a protein
49 fusion between a thermosensitive target protein in the N-
50 terminus and a thermostable kanamycin nucleotidyl trans-
51 ferase⁴ (Kat) in the C-terminus (Figure S1). This method has
52 proven useful for the isolation of thermostable variants of
53 human interferons and enzymes for biocatalysis, such as lipase
54 A from *Bacillus subtilis*, formate dehydrogenase from
55 *Pseudomonas* sp. 101,⁵ and more recently, the esterase I from
56 *Pseudomonas fluorescens*.⁶

In the course of generating thermostable variants of the 57
58 latter enzyme, we encountered a large number of false positives
59 that we attributed to having used a dimeric folding interference
60 reporter, such as Kat. Therefore, we evolved the monomeric,

Received: January 31, 2021

Revised: March 21, 2021

61 moderately thermostable hygromycin B phosphotransferase
62 variant (Hph5) from *Escherichia coli* reported by Nakamura et
63 al.⁷ Hph5 accumulated five amino acid substitutions that
64 allowed *T. thermophilus* to grow at temperatures up to 67 °C.
65 However, lower transformation efficiency of this marker in
66 *Thermus* had been reported at that temperature,⁷ compromising
67 the throughput of our selection method as well as limiting
68 the selection pressure, i.e. temperature, that can be applied.

69 Consequently, in this work we engineered a bespoke, highly
70 thermostable, monomeric folding reporter (Hph17) and used
71 it to stabilize the *E. coli* 2-keto-3-deoxy-1-rhamnonate aldolase
72 (YfaU). YfaU is a class II pyruvate aldolase that accepts a wide
73 range of electrophiles, and even though the natural
74 nucleophilic substrate is pyruvate, it can also use homologous
75 ketoacids. The aldol addition of pyruvate or homologues to a
76 wide variety of *N*-carboxybenzyl-amino aldehydes are
77 especially relevant since the resulting aldol adducts are
78 intermediates of new proline, pyrrolizidine-3-carboxylic acid,
79 pipercolic acid, and β -hydroxy- γ -amino acid derivatives.^{8,9}
80 Moreover, YfaU plays an important role in the biocatalytic
81 cascade for the synthesis of the noncanonical amino acid (*S*)-2-
82 amino-4-hydroxybutanoic acid (*L*-homoserine). YfaU can
83 synthesize (*S*)- or (*R*)-2-amino-4-hydroxybutanoic acid with
84 *ee* values of >99% using pyruvate and formaldehyde as
85 substrates, and a transaminase provides pyruvate from alanine,
86 thus *L*-homoserine is produced using formaldehyde and alanine
87 as sole and inexpensive starting materials¹⁰

88 ■ RESULTS AND DISCUSSION

89 **Library Generation and Selection of Hph Variants.** In
90 order to improve the stability of Hph5 for its use as a folding
91 interference reporter, the *hph5* gene was randomized by error-
92 prone PCR (epPCR) in the presence of 0.2 mM Mn²⁺ to
93 introduce 3–6 nucleotide replacements per gene, which
94 represent between 2 and 5 amino acid changes, in good
95 agreement with most directed evolution studies.¹¹ The epPCR
96 Hph5 library was generated in *E. coli* and then transformed in
97 *T. thermophilus* for selection. The generated *E. coli* library of
98 4.5×10^4 individuals was selected at 70 °C and 100 μ g/mL of
99 hygromycin B (HygB), at which transformants expressing
100 parental Hph5 could not grow (Figure S2). Under permissive
101 conditions (60 °C and 100 μ g/mL of HygB), 9961 CFU/ng
102 plasmid were obtained, while under selection pressure (70 °C
103 and 100 μ g/mL of HygB) only 32 CFU/ng of plasmid were
104 selected, which represents a selection factor of 0.32%. Because
105 of the high number of transformants obtained under those
106 conditions, the temperature had to be subsequently increased
107 to 71 °C, leading to 2 CFU/ng plasmid and a selection factor
108 of 0.02%.

109 Twenty randomly selected clones were verified for HygB
110 resistance using a serial dilution assay at 71 °C (Figure S3, A).
111 A particular variant (Hph17) harboring five changes (R61H,
112 S86G, Q96P, A185V, and V322E) was found four times in the
113 pool and enabled growth of *Thermus* even at 74 °C (Figure
114 S3B). It seems unlikely that all of these four individuals
115 originated independently during epPCR, but their recurrence
116 is likely a natural consequence of library construction in *E. coli*
117 prior to selection in *Thermus*. Most importantly, unlike the *in*
118 *vivo* mutagenesis used by Nakamura to generate Hph5,⁷ *in vitro*
119 mutagenesis by epPCR likely enabled the creation of a larger
120 and more diverse sequence space, from which a fitter variant
121 can be selected. In fact, it took a combination of natural
122 evolution, DNA shuffling, and random amino acid duplications

to confer a similar degree of thermostability to a hygromycin
123 phosphotransferase from *Streptomyces hygroscopicus* (Hyg10).¹² 124

Kinetic, Thermodynamic, and Structural Character-
ization of Hph17. The mutations of the moderately
126 thermostable Hph5 were mostly situated in the hydrophobic
127 core.¹³ In contrast, three out of the four thermostabilizing
128 positions mutated in the Hph17 variant (R61H, S86G, Q96P,
129 and A185V) are found on the protein surface, except A185V, 130
which is located in a hydrophobic core (Figure 1), reducing 131 f1

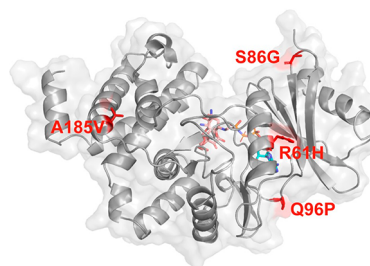


Figure 1. Location of stabilizing mutations in Hph17 variant. Amino acid substitutions are shown as red sticks. Substrates hygromycin B (HygB) and phosphoaminophosphonic acid-adenylate ester (ANP) are depicted as sticks in CPK colors with carbon atoms in salmon and cyan, respectively.

the distance between the adjacent β -strands and contributing
toward compactness.¹⁴ On the other hand, residue 96 is placed
in a loop and substitution of Gln to Pro in a loop diminishes
the RMSD of that region, contributing to the overall
stabilization of the enzyme. Finally, A185V strengthens the
hydrophobic interactions and increases the protein packing³
since Val is bulkier than Ala.

As shown in Table 1, both the catalytic constant, k_{cat} , and
the efficiency for ATP, $K_{M,ATP}$, remained unaltered in Hph17
compared with the parental enzyme. However, $K_{M,HygB}$, was
2.4-fold higher for Hph17 respect to that of Hph5, with a
consequent reduction in the catalytic efficiency. Regarding
thermostability, the melting temperature of Hph17 was 1.5 °C
higher than that of Hph5, while its half-life at 65 °C doubled,
with the main contributions toward this enhancement
originating from replacements S86G and Q96P. Increases in
kinetic stability usually suggest that these mutations may
interfere with an initial step on the path toward the irreversible
unfolded state, thus avoiding further global unfolding.^{15,16}
Therefore, we used constraint network analysis (CNA), to
simulate protein unfolding.¹⁷ As shown in Figure 2, positions
Ser86 and Gln96 were some of the most flexible *loci* in the
protein (highest r_i values), congruently with the postulated
“hinge” function of neighboring Val98.¹³ Thus, replacing Ser86
and Gln96 would restrict local movements leading to unfolded
states by irreversible denaturation, which might explain the
increase in half-life of variants S86G and Q96P (Table 1).

When Hph5 was evolved from Hph, a marked increase in
thermodynamic stability was observed, despite the lack of a
clear structural explanation.^{13,18} However, neither Hph17 nor
the individual variants showed an increase in melting
temperature (T_m) over the parental Hph5, suggesting that a
further increase of protein rigidity significant enough to gain
thermodynamic stability could be detrimental for the enzyme
activity. This result is not incompatible with the putative
higher protein stability *in vivo*, which could be enhanced by
factors such as the molecular crowding and compatible solutes

Table 1. Kinetic^a and Stability Parameters for Hph5, Hph17, and the Segregated Variants Containing the Amino Acid Replacements of Hph17^b

Hph variant	$K_{M,HygB}$ (mM)	$K_{M,ATP}$ (mM)	k_{cat} (min ⁻¹)	$k_{cat}/K_{M,HygB}$ (min ⁻¹ mM ⁻¹)	$k_{cat}/K_{M,ATP}$ (min ⁻¹ mM ⁻¹)	T_m (°C)	half-life (min)	k_d (min ⁻¹)
Hph5	0.29 ± 0.03	0.37 ± 0.02	2984 ± 72	10290	8065	58.2 ± 0.1	2.2 ± 0.4	0.33 ± 0.06
Hph17	0.7 ± 0.10	0.39 ± 0.03	2847 ± 153	4067	7300	59.7 ± 0.1	7 ± 3	0.12 ± 0.05
R61H	0.84 ± 0.09	0.46 ± 0.04	3578 ± 133	4260	7778	59.5 ± 0.1	2.2 ± 0.2	0.31 ± 0.03
S86G	0.50 ± 0.07	0.55 ± 0.03	3202 ± 44	6404	5822	59.6 ± 0.3	4.7 ± 0.9	0.15 ± 0.04
Q96P	0.41 ± 0.03	0.31 ± 0.03	3555 ± 76	8671	11468	59.5 ± 0.2	3.0 ± 0.1	0.23 ± 0.01
A185V	0.39 ± 0.06	0.32 ± 0.02	2672 ± 108	6851	8350	57.9 ± 0.1	1.6 ± 0.2	0.43 ± 0.06
V322E	0.57 ± 0.09	0.39 ± 0.02	3196 ± 145	5607	8195	59.1 ± 0.4	1.9 ± 0.4	0.38 ± 0.08

^aSteady-state kinetic constants were determined at 60 °C. ^bHalf-lives and deactivation constants (K_d) were determined at 65 °C. Values represent the mean ± standard deviation of three independent determinations.

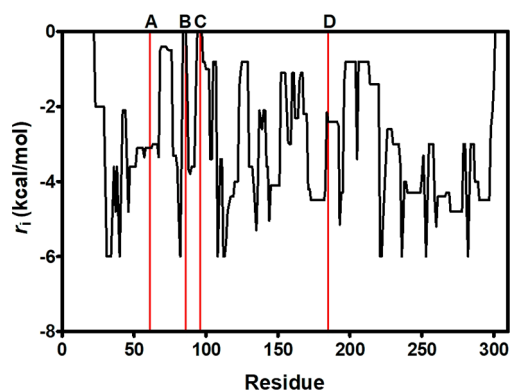


Figure 2. Constraint network analysis of Hph5. Lines indicate the four amino acid replacements in Hph17 (line A corresponds to position Arg61; line B, Ser86; line C, Gln96; and line D, Ala185) that can be mapped in the homology model.

169 of the *Thermus* cytoplasm¹⁹ whereas T_m determinations are
170 carried out with the protein in buffer. In contrast, different
171 scaffolds, such as Hyg10, have been evolved to both higher T_m
172 (12.2 °C) and specific activity (2-fold) at the optimum activity
173 temperature.¹² However, the sequence identity of the Hyg10
174 and Hph proteins is approximately 30%, and their activity is
175 not identical, as Hyg10 phosphorylates HygB in a different
176 hydroxyl group.

177 The folding free energy of the mutants ($\Delta\Delta G$) was
178 estimated using FoldX. The $\Delta\Delta G$ values obtained were 0.78,
179 0.50, -0.92, 0.21, and 0.58 kcal/mol for the single variants
180 R61H, S86G, Q96P, A185V, and the multiple mutant
181 containing R61H, S86G, Q96P, and A185V, respectively. In
182 this case, FoldX cannot predict correctly the found mutants
183 given the very low differences in T_m between variants, and the
184 standard deviation of predicted values (between 1.0 and 1.7
185 kcal/mol).²

186 **Library Generation and Selection of Thermostable**
187 **YfaU Variants.** Hph17 was used as a folding interference
188 reporter to engineer higher stability in YfaU (Figures 3 and
189 S1). The class II pyruvate aldolase, YfaU, was mutagenized by
190 epPCR in the presence of 0.3 mM Mn²⁺. The library sequences



Figure 3. Gene fusion of *yfaU* to *hph17*, expressed under the promoter *slpA* (*slpAp*).

analyzed contained between 1 and 8 nucleotide replacements, 191
i.e., 1–6 amino acid substitutions. The generated library of 1.5 192
 $\times 10^5$ individuals was selected in *T. thermophilus* at 67 °C and 193
100 $\mu\text{g}/\text{mL}$ of HygB, conditions under which the trans- 194
formants expressing the wild-type YfaU (YfaU-wt) could not 195
grow (Figure S4). 196

Due to the large number of variants selected, 54 unique 197
clones were randomly picked to perform a dilution assay on 198
plate at 67 °C (Figure S5). The 12 variants with the highest 199
growth (variants 2, 8, 14, 15, 48, 50, 63, 66, 70, 99, 103, and 200
105) were chosen for subsequent sequencing and character- 201
ization. 202

Characterization of Thermostable YfaU Variants. The 203
12 selected YfaU variants and YfaU-wt were cloned into 204
pET28b, transformed in *E. coli* BL21, and expressed using 205
autoinduction medium at 20 °C. The solubility of these 206
variants was checked by SDS-PAGE; supernatant and pellet 207
were run separately (Figure S6). Only four of the variants 208
showed the presence of the protein in the supernatant fraction. 209
The lack of solubility of these putative thermostable YfaU 210
variants could arise from differences between the context in 211
which they were selected and produced, i.e., a fusion protein in 212
a thermophile host vs a standalone protein in a mesophile. 213
Also, the low solubility of YfaU has been previously described, 214
requiring expression in fusion with either dihydrofolate 215
reductase (DHFR) or maltose binding protein (MBP) at the 216
N-terminus.¹⁰ 217

These four YfaU variants and YfaU-wt were purified by 218
immobilized metal affinity chromatography (IMAC), and their 219
 T_m values were measured. Variants 2 (H49Q and G118D) and 220
14 (G39D and I73F) showed T_m s 8.5 and 5.5 °C lower than 221
YfaU-wt, while variants 99 (L4F, G90S, Q107R, Q141L, 222
F215L, A252E, F254I, and I263 K) and 103 (V122F, P187T, 223
and P261Q) increased their T_m s by 2.0 and 2.9 °C, 224
respectively, compared with YfaU-wt. However, the assessment 225
of variants 99 and 103 using a straightforward retro-aldol 226
reaction showed a 150- and 120-fold reduction in activity, 227
respectively (Table 2). These results agree with previous 228
studies of randomized libraries, in which an increase in thermal 229
stability resulted in lower activity,^{20,21} due to a gradual loss of 230
flexibility as the number of mutations increases.²² Furthermore, 231
selection by folding interference is an activity-independent 232
process, which may be convenient in cases where a functional 233
selection is either complex or impossible⁵ but, in this case, led 234
to lower activity values due to lack of selective pressure toward 235
function. 236

To remediate the observed activity–stability trade-off, the 237
amino acid replacements of these two variants were segregated 238

Table 2. Specific Retro-Aldol Activity,^a T_m , and Half-Life^b of YfaU Variants

YfaU variant	specific retro-aldol activity (U/mg)	T_m (°C)	half-life (min)
wild-type	60 ± 1	60.5 ± 0.0	0.9 ± 0.1
YfaU99	0.4 ± 0.2	62.5 ± 1.0	nm
YfaU103	0.5 ± 0.3	63.4 ± 0.2	nm
Q107R	48 ± 7	69.4 ± 0.2	14 ± 1
Q141L	62 ± 6	62.7 ± 0.2	3.0 ± 0.3

^aSpecific activity was determined at 25 °C. ^bHalf-life was measured at 60 °C. Values represent the mean and the standard deviation of three independent determinations. nm: nonmeasurable.

Table 4. Estimated Values of Operational Stability Decay Rate Constants (k_d) and the Corresponding Half-Life Times in a Batch Reactor at 25 °C^a

YfaU variant	k_d (h ⁻¹)	half-life (h)
wild-type	0.144 ± 0.013	4.8 ± 0.4
Q107R	0.068 ± 0.006	10.2 ± 0.9
Q141L	0.061 ± 0.006	11 ± 1

^aValues represent the mean and the standard deviation of three independent determinations.

enzyme activity in the reactor in the presence of substrate, cofactor, and products.²⁴

Structure–Function Analysis of YfaU Q107R and Q141L

To investigate the reason why both mutants were more thermostable, homology models of Q107R and Q141L were built using the crystal structures of YfaU-wt (PDB: 2VWS and 2VWT). YfaU presents a hexameric assembly composed by a trimer (3-fold axis) of (β/α)₈ barrel dimers (2-fold axis). Since the 2-fold related subunits superpose with an RMSD of 0.25 Å²⁵ and residues Gln107 and Gln141 are not involved in the interaction between subunits, only the 3-fold related subunits were considered for the analysis (Figure S9). The replacement Q107R decreased the number of H-bonds with the replaced residue or with other amino acids in its hydrogen bond network. Similar results were found for the mutant Q141L (Figure 4).

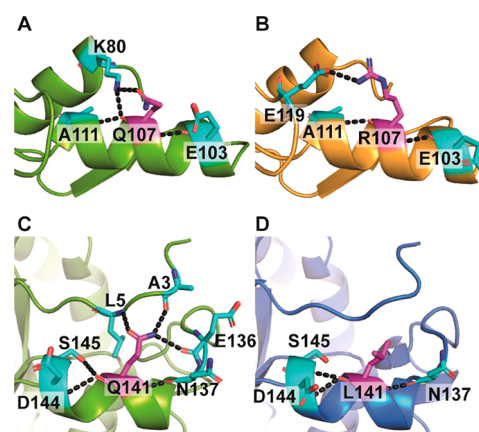


Figure 4. Hydrogen bonds formed between residues 107 and 141 with their surrounding residues, respectively. A. Residue Gln107 of YfaU-wt. B. Residue Arg107 of variant Q107R. C. Residue Gln141 of YfaU-wt. D. Residue Leu141 of variant Q141L. Target residues are depicted in magenta sticks in CPK colors, while residues which form hydrogen bonds are illustrated as cyan sticks.

Rigidity index (r_i) from the CNA algorithm was also used to monitor the degree of rigidity of the residues from YfaU-wt (Figure 5). As previously described, only the trimeric assembly

and their T_m s and specific activities were measured individually (Table 2). Only variants Q107R and Q141L (both derived from variant 99) increased their T_m s by 8.9 and 2.2 °C, respectively, compared to YfaU-wt while increasing or maintaining the retro-aldol activities of the wild-type enzyme. In addition, the half-lives of Q107R and Q141L were 16- and 3.3-fold higher compared to YfaU-wt, respectively. Considering that only 0.01–0.5% of random mutations are beneficial,²³ the increase in thermostability of Q107R seems to arise from a truly beneficial mutation, and the rest of the mutations in variant 99 have a deleterious or neutral effect on enzyme stability.

Performance of YfaU Q107R and Q141L in the Aldol Addition of Pyruvate to Formaldehyde. To test the proficiency of the best YfaU variants in a biocatalytically relevant reaction, the aldol addition of pyruvate to formaldehyde was assayed, modeled and the steady-state kinetic parameters were calculated for YfaU-wt, Q107R, and Q141L (Table 3 and Figure S7).

The ca. 2-fold increase in k_{cat} and decrease of K_M for both substrates for variant Q141L resulted in a 3.1- and 6.8-fold increase in catalytic efficiency (k_{cat}/K_M) for formaldehyde and pyruvate, respectively. Moreover, K_i for both substrates increased. Variant Q107R showed better turnover and similar K_M values compared to YfaU-wt, while K_i for formaldehyde decreased.

The operational stability of the Q107R and Q141L variants in this reaction was evaluated in a batch reactor. Assuming that the decay in operational stability can be described by first order kinetics (Figure S8), the calculated deactivation constants (k_d) for variants Q107R and Q141L are approximately 2-fold lower than for YfaU-wt (Table 4). Both variants showed similar values in terms of operational stability (k_d and half-life), which contrasts with their differences in kinetic thermostability, where Q107R showed a half-life at 60 °C almost 5-fold higher than Q141L (Table 2). These differences between kinetic and operational stability could be explained by the fact that half-life at high temperature considers only the stability of the protein molecule in buffer, while operational stability considers

Table 3. Steady-State Kinetic Parameters for the Aldol Addition of Pyruvate and Formaldehyde Catalyzed by YfaU-wt, Q107R, and Q141L^a

YfaU variant	k_{cat} (min ⁻¹)	$K_{M,formaldehyde}$ (mM)	$k_{cat}/K_{M,formaldehyde}$ (min ⁻¹ mM ⁻¹)	$K_{i,formaldehyde}$ (mM)	$K_{M,pyruvate}$ (mM)	$k_{cat}/K_{M,pyruvate}$ (min ⁻¹ mM ⁻¹)	$K_{i,pyruvate}$ (mM)
wild-type	113 ± 40	24 ± 4	4.71	95 ± 14	209 ± 83	0.54	47 ± 18
Q107R	180 ± 53	26 ± 6	6.92	75 ± 16	61 ± 20	2.95	46 ± 15
Q141L	242 ± 28	17 ± 2	14.2	113 ± 12	66 ± 10	3.67	151 ± 22

^aValues represent the mean and the standard deviation of three independent determinations.

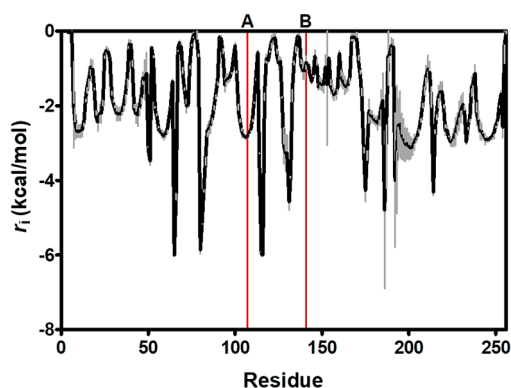


Figure 5. Rigidity index (r_i) for YfaU-wt calculated by CNA. Lines indicate the amino acid replacements (line A corresponds to position 107 and line B, position 141). Since YfaU is a homotrimer, r_i has been averaged for the same residue of each chain. The mean value is shown in black, and the standard deviations are in gray.

297 was considered for structural analysis. Considering this and
 298 since CNA does not relate residues from different chains, r_i has
 299 been averaged from the three different chains. According to
 300 CNA, with a r_i value of -2.8 kcal/mol, residue Gln107 is not in
 301 a flexible region of the protein. However, residue Gln141 has a
 302 r_i value of -0.84 kcal/mol, which implies a certain degree of
 303 flexibility in this region.

304 Finally, FoldX calculations were carried out to estimate the
 305 folding free energy of the mutants ($\Delta\Delta G$). Q107R caused a
 306 $\Delta\Delta G$ of -2.55 kcal/mol. Considering $\Delta\Delta G$ from FoldX and
 307 the general rule that correlates ΔG_{unfold} and ΔT_m^2 , the
 308 corresponding empirical ΔT_m would be 9.2 °C, which is
 309 similar to the experimental ΔT_m , 8.9 °C. By contrast, $\Delta\Delta G$ of
 310 variant Q141L was 0.08 kcal/mol, which would represent a
 311 ΔT_m of -0.3 °C, while the experimental ΔT_m was 2.2 °C.

312 Considering the output of the chosen methods and
 313 algorithms used for structure–function analysis, we could
 314 identify beneficial mutations using our screening system, which
 315 would not be made easily evident by bioinformatics tools.
 316 However, the folding interference principle in *T. thermophilus*
 317 allowed the identification of these stabilizing positions, in
 318 consonance with a recent study in which stabilizing positions
 319 were identified in the esterase I from *Pseudomonas fluorescens*
 320 also by folding interference, using the kanamycin nucleotidyl
 321 transferase gene as folding reporter instead.⁶

322 ■ CONCLUSIONS

323 The improvement of hygromycin B phosphotransferase
 324 (Hph17) enabled the thermal stabilization of the pyruvate
 325 aldolase from *E. coli* YfaU. The only two selected variants that
 326 were expressed in soluble form, YfaU99 and 103, showed
 327 higher T_m than the wild-type protein, 2.0 and 2.9 °C,
 328 respectively, at the cost of a lower specific activity. However,
 329 the low solubility issue can be solved using complementary
 330 rational design strategies, such as specific solubility-enhancing
 331 algorithms or back-to-consensus mutations that restore
 332 conserved amino acids, which usually yield active and more
 333 soluble proteins.^{24,26,27}

334 With the aim of knowing the effect of individual mutations
 335 both in enzyme activity and stability, all mutations were
 336 segregated and characterized individually. The Q107R and
 337 Q141L replacements conferred higher kinetic and thermody-
 338 namic stability. Especially interesting is the case of variant

Q107R, with an increase of 8.9 °C in T_m , 16-fold longer half-
 life, and similar kinetic constants than YfaU-wt. Regarding
 variant Q141L, the improvement in stability was much more
 modest, but this variant had better turnover, affinity, and lower
 substrate inhibition compared to the wild-type.

YfaU is a relevant enzyme for biocatalysis, allowing for
 instance the synthesis of L-homoserine using alanine and up to
 3 M formaldehyde, when coupled with a transaminase.¹⁰ Our
 highly active and thermostable Q107R and Q141L variants
 have twice the operational stability of YfaU-wt in the synthesis
 of 4-hydroxy-2-oxobutanoate, which would allow a longer-term
 usage in this cascade reaction, with the consequent reduction
 in the cost of the process.

■ ASSOCIATED CONTENT

Supporting Information

The Supporting Information is available free of charge at
<https://pubs.acs.org/doi/10.1021/acssuschemeng.1c00699>.

Tables, figures, and experimental procedures (PDF)

■ AUTHOR INFORMATION

Corresponding Author

Aurelio Hidalgo – Department of Molecular Biology, Center
 of Molecular Biology “Severo Ochoa” (UAM-CSIC),
 Autonomous University of Madrid, 28049 Madrid, Spain;
 orcid.org/0000-0001-5740-5584; Email: ahidalgo@
 cbm.csic.es

Authors

Sandra Bosch – Department of Molecular Biology, Center of
 Molecular Biology “Severo Ochoa” (UAM-CSIC),
 Autonomous University of Madrid, 28049 Madrid, Spain

Esther Sanchez-Freire – Department of Molecular Biology,
 Center of Molecular Biology “Severo Ochoa” (UAM-CSIC),
 Autonomous University of Madrid, 28049 Madrid, Spain

María Luisa del Pozo – Department of Molecular Biology,
 Center of Molecular Biology “Severo Ochoa” (UAM-CSIC),
 Autonomous University of Madrid, 28049 Madrid, Spain

Morana Česnik – University of Zagreb, Faculty of Chemical
 Engineering and Technology, HR-10000 Zagreb, Croatia

Jaime Quesada – Department of Molecular Biology, Center of
 Molecular Biology “Severo Ochoa” (UAM-CSIC),
 Autonomous University of Madrid, 28049 Madrid, Spain

Diana M. Mate – Department of Molecular Biology, Center of
 Molecular Biology “Severo Ochoa” (UAM-CSIC),
 Autonomous University of Madrid, 28049 Madrid, Spain

Karel Hernández – Institute of Advanced Chemistry of
 Catalonia, Biotransformation and Bioactive Molecules
 Group, Spanish National Research Council (IQAC–CSIC),
 08034 Barcelona, Spain

Yuyin Qi – Prozomix Ltd, Haltwhistle NE49 9HN,
 Northumberland, United Kingdom

Pere Clapés – Institute of Advanced Chemistry of Catalonia,
 Biotransformation and Bioactive Molecules Group, Spanish
 National Research Council (IQAC–CSIC), 08034
 Barcelona, Spain; orcid.org/0000-0001-5541-4794

Đurda Vasić-Rački – University of Zagreb, Faculty of
 Chemical Engineering and Technology, HR-10000 Zagreb,
 Croatia

Zvezdana Findrik Blažević – University of Zagreb, Faculty of
 Chemical Engineering and Technology, HR-10000 Zagreb,
 Croatia

398 José Berenguer – Department of Molecular Biology, Center of
399 Molecular Biology “Severo Ochoa” (UAM-CSIC),
400 Autonomous University of Madrid, 28049 Madrid, Spain

401 Complete contact information is available at:
402 <https://pubs.acs.org/10.1021/acssuschemeng.1c00699>

403 Author Contributions

404 S.B. performed the experiments on library generation,
405 selection, and characterization of Hph and YfaU variants,
406 compiled and analyzed all data, and wrote the first version of
407 the manuscript. J.Q. did the characterization of the Hph single
408 variants. M.L.d.P. contributed to the experiments on library
409 generation and selection of YfaU. E.S.-F. contributed to the
410 characterization of the YfaU variants. M.C. performed the
411 modeling of the steady-state kinetic parameters and opera-
412 tional stability of YfaU. Y.Q. did the production of pyruvate
413 kinase. S.B. and D.M.M. contributed to data analysis, figure
414 design, writing, and editing of the manuscript. K.H., P.C., D.V.-
415 R. Z.F.B., and J.B. contributed to manuscript writing. A.H.
416 conceived and supervised the project and wrote the final
417 version of the manuscript. All authors have given approval to
418 the final version of the manuscript.

419 Notes

420 The authors declare no competing financial interest.

421 ■ ACKNOWLEDGMENTS

422 This work has been funded through the European Union’s
423 Research and Innovation program Horizon 2020 through grant
424 agreement no. 635595 (CarbaZymes) and by the Spanish
425 Ministry of Economy and Competitiveness through grant BIO-
426 2013-44963R. Institutional grants from the Fundación Ramón
427 Areces and Banco Santander to the CBMSO are also
428 acknowledged. S.B. is the recipient of a Ph.D. fellowship
429 from UAM. D.M.M. was supported by a Research Talent
430 Attraction contract from the Community of Madrid. A
431 generous allocation of computing time at the Scientific
432 Computation Center of the UAM (CCC-UAM) is also
433 acknowledged.

434 ■ REFERENCES

435 (1) Woodley, J. M. Protein Engineering of Enzymes for Process
436 Applications. *Curr. Opin. Chem. Biol.* **2013**, *17* (2), 310–316.
437 (2) Buß, O.; Rudat, J.; Ochsenreither, K. FoldX as Protein
438 Engineering Tool: Better Than Random Based Approaches? *Comput.*
439 *Struct. Biotechnol. J.* **2018**, *16*, 25–33.
440 (3) Mate, D. M.; Gonzalez-Perez, D.; Mateljak, I.; Gomez de Santos,
441 P.; Vicente, A. L.; Alcalde, M. The Pocket Manual of Directed
442 Evolution: Tips and Tricks. In *Biotechnology of Microbial Enzymes:*
443 *Production, Biocatalysis and Industrial Applications* **2017**, 185–213.
444 (4) Matsumura, M.; Aiba, S. Screening for Thermostable Mutant of
445 Kanamycin Nucleotidyltransferase by the Use of a Transformation
446 System for a Thermophile, *Bacillus Stearothermophilus*. *J. Biol. Chem.*
447 **1985**, *260* (28), 15298–15303.
448 (5) Chautard, H.; Blas-Galindo, E.; Menguy, T.; Grand’Moursel, L.;
449 Cava, F.; Berenguer, J.; Delcourt, M. An Activity-Independent
450 Selection System of Thermostable Protein Variants. *Nat. Methods*
451 **2007**, *4* (11), 919–921.
452 (6) Mate, D. M.; Rivera, N. R.; Sanchez-Freire, E.; Ayala, J. A.;
453 Berenguer, J.; Hidalgo, A. Thermostability Enhancement of the
454 *Pseudomonas Fluorescens* Esterase I by in Vivo Folding Selection in
455 *Thermus Thermophilus*. *Biotechnol. Bioeng.* **2020**, *117* (1), 30–38.
456 (7) Nakamura, A.; Takakura, Y.; Kobayashi, H.; Hoshino, T. In Vivo
457 Directed Evolution for Thermostabilization of *Escherichia Coli*
458 Hygromycin B Phosphotransferase and the Use of the Gene as a

Selection Marker in the Host-Vector System of *Thermus* 459
Thermophilus. *J. Biosci. Bioeng.* **2005**, *100* (2), 158–163. 460
(8) Hernández, K.; Gómez, A.; Joglar, J.; Bujons, J.; Parella, T.; 461
Clapés, P. 2-Keto-3-Deoxy-1-Rhamnonate Aldolase (YfaU) as Catalyst 462
in Aldol Additions of Pyruvate to Amino Aldehyde Derivatives. *Adv.* 463
Synth. Catal. **2017**, *359* (12), 2090–2100. 464
(9) Hernandez, K.; Joglar, J.; Bujons, J.; Parella, T.; Clapes, P. 465
Nucleophile Promiscuity of Engineered Class II Pyruvate Aldolase 466
YfaU from *E. Coli*. *Angew. Chem., Int. Ed.* **2018**, *57* (14), 3583–3587. 467
(10) Hernandez, K.; Bujons, J.; Joglar, J.; Charnock, S. J.; 468
Domínguez De María, P.; Fessner, W. D.; Clapés, P. Combining 469
Aldolases and Transaminases for the Synthesis of 2-Amino-4- 470
Hydroxybutanoic Acid. *ACS Catal.* **2017**, *7* (3), 1707–1711. 471
(11) Wong, T.; Zhurina, D.; Schwaneberg, U. The Diversity 472
Challenge in Directed Protein Evolution. *Comb. Chem. High* 473
Throughput Screening **2006**, *9* (4), 271–288. 474
(12) Sugimoto, N.; Takakura, Y.; Shiraki, K.; Honda, S.; Takaya, N.; 475
Hoshino, T.; Nakamura, A. Directed Evolution for Thermostabiliza- 476
tion of a Hygromycin B Phosphotransferase from *Streptomyces* 477
Hygroscopicus. *Biosci., Biotechnol., Biochem.* **2013**, *77* (11), 2234– 478
2241. 479
(13) Iino, D.; Takakura, Y.; Fukano, K.; Sasaki, Y.; Hoshino, T.; 480
Ohsawa, K.; Nakamura, A.; Yajima, S. Crystal Structures of the 481
Ternary Complex of APH(4)-Ia/Hph with Hygromycin B and an 482
ATP Analog Using a Thermostable Mutant. *J. Struct. Biol.* **2013**, *183* 483
(1), 76–85. 484
(14) Bednar, D.; Beerens, K.; Sebestova, E.; Bendl, J.; Khare, S.; 485
Chaloupkova, R.; Prokop, Z.; Brezovsky, J.; Baker, D.; Damborsky, J. 486
FireProt: Energy- and Evolution-Based Computational Design of 487
Thermostable Multiple-Point Mutants. *PLoS Comput. Biol.* **2015**, *11* 488
(11), e1004556. 489
(15) Bommarius, A. S.; Paye, M. F. Stabilizing Biocatalysts. *Chem.* 490
Soc. Rev. **2013**, *42* (15), 6534–6565. 491
(16) Brouns, S. J. J.; Wu, H.; Akerboom, J.; Turnbull, A. P.; De Vos, 492
W. M.; Van Der Oost, J. Engineering a Selectable Marker for 493
Hyperthermophiles. *J. Biol. Chem.* **2005**, *280* (12), 11422–11431. 494
(17) Krüger, D. M.; Rathi, P. C.; Pflieger, C.; Gohlke, H. CNA Web 495
Server: Rigidity Theory-Based Thermal Unfolding Simulations of 496
Proteins for Linking Structure, (Thermo-)Stability, and Function. 497
Nucleic Acids Res. **2013**, *41*, 340–348. 498
(18) Nakamura, A.; Takakura, Y.; Sugimoto, N.; Takaya, N.; Shiraki, 499
K.; Hoshino, T. Enzymatic Analysis of a Thermostabilized Mutant of 500
an *Escherichia Coli* Hygromycin B Phosphotransferase. *Biosci.,* 501
Biotechnol., Biochem. **2008**, *72* (9), 2467–2471. 502
(19) Borges, N.; Ramos, A.; Raven, N. D. H.; Sharp, R. J.; Santos, H. 503
Comparative Study of the Thermostabilizing Properties of Man- 504
nosylglycerate and Other Compatible Solutes on Model Enzymes. 505
Extremophiles **2002**, *6* (3), 209–216. 506
(20) Kurahashi, R.; Tanaka, S. i.; Takano, K. Activity-Stability 507
Trade-off in Random Mutant Proteins. *J. Biosci. Bioeng.* **2019**, *128* (4), 508
405–409. 509
(21) Tokuriki, N.; Stricher, F.; Serrano, L.; Tawfik, D. S. How 510
Protein Stability and New Functions Trade Off. *PLoS Comput. Biol.* 511
2008, *4* (2), 35–37. 512
(22) Modarres, H. P.; Mofrad, M. R.; Sanati-Nezhad, A. Protein 513
Thermostability Engineering. *RSC Adv.* **2016**, *6* (116), 115252– 514
115270. 515
(23) Bloom, J. D.; Arnold, F. H. In the Light of Directed Evolution: 516
Pathways of Adaptive Protein Evolution. *Proc. Natl. Acad. Sci. U. S. A.* 517
2009, *106* (Supplement1), 9995–10000. 518
(24) Bommarius, A. S.; Drauz, K.; Klenk, H.; Wandrey, C. 519
Operational Stability of Enzymes. Acylase-Catalyzed Resolution of 520
N-Acetyl Amino Acids to Enantiomerically Pure L-Amino Acids. *Ann.* 521
N. Y. Acad. Sci. **1992**, *672*, 126–136. 522
(25) Rea, D.; Hovington, R.; Rakus, J. F.; Gerlt, J. A.; Fülöp, V.; 523
Bugg, T. D. H.; Roper, D. I. Crystal Structure and Functional 524
Assignment of YfaU, a Metal Ion Dependent Class II Aldolase from 525
Escherichia Coli K12. *Biochemistry* **2008**, *47* (38), 9955–9965. 526

- 527 (26) Kazlauskas, R. Engineering More Stable Proteins. *Chem. Soc.*
528 *Rev.* **2018**, *47* (24), 9026–9045.
- 529 (27) Mayer, S.; Rüdiger, S.; Ang, H. C.; Joerger, A. C.; Fersht, A. R.
530 Correlation of Levels of Folded Recombinant P53 in Escherichia Coli
531 with Thermodynamic Stability in Vitro. *J. Mol. Biol.* **2007**, *372* (1),
532 268–276.